Endothelial infection with KSHV genes in vivo reveals that *vGPCR* initiates Kaposi's sarcomagenesis and can promote the tumorigenic potential of viral latent genes

Silvia Montaner,[1,6] Akrit Sodhi,[1,3,6] Alfredo Molinolo,[1] Thomas H. Bugge,[2] Earl T. Sawai,[3] Yunsheng He,[4] Yi Li,[5] Patricio E. Ray,[4] and J. Silvio Gutkind[1,*]

[1]Cell Growth Regulation Section
[2]Proteases and Tissue Remodeling Unit
Oral and Pharyngeal Cancer Branch, National Institute of Dental and Craniofacial Research, National Institutes of Health, Bethesda, Maryland 20892
[3]Department of Medical Pathology and Comparative Pathology Graduate Group, University of California at Davis, Davis, California 95616
[4]Research Center for Molecular Physiology, Children's National Medical Center and The George Washington University, Washington DC 20010
[5]Memorial Sloan-Kettering Cancer Center, 1275 York Avenue, New York, New York 10021
[6]These authors contributed equally to this work.
*Correspondence: sg39v@nih.gov

Summary

The Kaposi's sarcoma herpesvirus (KSHV) has been identified as the etiologic agent of Kaposi's sarcoma (KS), but initial events leading to KS development remain unclear. Characterization of the KSHV genome reveals the presence of numerous potential oncogenes. To address their contribution to the initiation of the endothelial cell-derived KS tumor, we developed a novel transgenic mouse that enabled endothelial cell-specific infection in vivo using virus expressing candidate KSHV oncogenes. Here we show that transduction of one gene, *vGPCR*, was sufficient to induce angioproliferative tumors that strikingly resembled human KS. Endothelial cells expressing vGPCR were further able to promote tumor formation by cells expressing KSHV latent genes, suggestive of a cooperative role among viral genes in the promotion of Kaposi's sarcomagenesis.

Introduction

Kaposi's sarcoma (KS) is an AIDS-defining illness and remains the most frequent tumor arising in HIV-infected patients (Boshoff and Chang, 2001; Moore and Chang, 2001). The clinical course of AIDS-related KS is variable, ranging from minimal stable disease to explosive growth, often involving the skin, oral mucosa, lymph nodes, and visceral organs, including the gastrointestinal tract, lung, liver, and spleen. Indeed, KS has recently emerged as one of the most common neoplasms among children and adult men in the developing world, and represents a significant cause of morbidity and mortality among the AIDS population (Mitsuyasu, 2000). Unfortunately, clinical management of KS has proven to be challenging. Today, despite extensive investigation into its molecular etiology, KS remains an incurable disease (Hermans, 2000; Mitsuyasu, 2000).

KS is a multifocal neovascular tumor characterized histologically by proliferating spindle cells, angiogenesis, erythrocyte-replete vascular slits, profuse edema, and a variable inflammatory cell infiltrate. The dominant cell of KS lesions, the spindle cell, elaborates a variety of proinflammatory and angiogenic factors and is considered the driving force in KS lesions (Ganem, 1997). The origin of the spindle cell remains unclear. Although believed to be of endothelial origin, its precise histogenesis, as well as the early events surrounding the initiation of the KS tumor, are still poorly understood (Flore et al., 1998; Ganem, 1997; Jenner and Boshoff, 2002). The recent discovery of the Kaposi's sarcoma associated herpesvirus (KSHV or HHV-8) has invigorated renewed interest in this enigmatic disease (Chang et al., 1994). This novel γ-herpesvirus is associated with all forms of KS (classic, iatrogenic, endemic, and AIDS-related), in addition to two other neoplastic disorders: primary effusion

SIGNIFICANCE

The study of Kaposi's sarcoma has been limited by the difficulty of passaging KSHV in vitro and the lack of appropriate animal models to study KS in vivo. To overcome these obstacles, we developed and characterized a mouse model system that mimics the infectious process by which KSHV targets endothelial cells in vivo, recapitulating the initiation of Kaposi's sarcomagenesis. Here we demonstrate a critical role for *vGPCR* in initiating KS tumor development. We also show that endothelial cells expressing vGPCR cooperate with cells expressing KSHV latent genes, promoting their tumorigenic potential through a paracrine mechanism. This animal model thus provides fundamental insight into the pathogenesis of KSHV and will be uniquely suited to further study the molecular events defining Kaposi's sarcoma.

lymphoma (PEL) and multicentric Castleman's disease (MCD). Of note, infection of primary human endothelial cells with purified KSHV induced cell transformation (Flore et al., 1998). However, further investigation revealed that the KSHV genome was present in only a subset of the transformed cells. These in vitro results correlate with what is observed in early human KS lesions, in which only a small percentage (10%) of endothelial and spindle cells are infected by KSHV (Dupin et al., 1999). These intriguing observations also suggest the involvement of a paracrine mechanism in KSHV sarcomagenesis.

Inspection of the KSHV genome reveals several candidate genes that bear potential for oncogenesis (Gruffat et al., 2000). Unfortunately, transmission of KSHV in vitro has met with limited success and, therefore, analysis of genomic deletion mutants is currently not feasible. The identification of potential KSHV oncogenes has relied primarily on their overexpression. A major caveat to these studies is that these genes are examined in vitro in cells that may not represent the natural target for KSHV infection; the results must therefore be interpreted cautiously.

To overcome current obstacles in examining the oncogenic potential of KSHV in endothelial cells in vivo, we engineered a transgenic mouse line expressing the avian leukosis virus (ALV) receptor, TVA (Bates et al., 1993; Young et al., 1993), under the control of the vascular endothelial cell-specific *TIE2* promoter (Schlaeger et al., 1997). Only mammalian cells engineered to express the *tva* transgene can be transduced by infection with ALV, thus enabling the somatic introduction of multiple genes in vivo, in a tissue-specific manner (Federspiel et al., 1994; Fisher et al., 1999; Orsulic et al., 2002). Using this model, we then examined the ability of individual KSHV genes to initiate KS development using ALV-derived recombinant retroviruses encoding candidate KSHV oncogenes. Despite prior studies suggesting that several latent genes—believed to be critical for KS progression—harbor transforming potential in vitro (Jenner and Boshoff, 2002), these genes do not appear to be sufficient to initiate endothelial cell transformation in vivo in our mouse model. However, inclusion of additional genes also suspected of playing a critical role in spindle cell growth and survival revealed that one gene, the constitutively active KSHV G protein-coupled receptor (*vGPCR*), when injected in isolation, potently induced Kaposi-like lesions in *TIE2-tva* mice. These tumors strikingly resembled human KS and expressed key histopathological and molecular hallmarks for this disease. Remarkably, endothelial cells expressing vGPCR were further able to promote the tumorigenic potential of cells expressing latent KSHV genes through a paracrine mechanism. These findings implicate *vGPCR* in both the initiation and promotion of KS tumor development and further suggest that this viral G protein-coupled receptor may be a key target in the development of pathogenesis-based therapies against KSHV.

Results

Characterization of *TIE2-tva* transgenic mice

To study the role of KSHV-encoded oncogenes in KS pathogenesis in vivo, we developed a TVA-based retroviral gene transfer system to specifically express candidate KSHV oncogenes in mouse endothelial cells. We engineered transgenic mice to express the avian retroviral receptor, TVA, under the control of the vascular endothelial cell-specific *TIE2* promoter. Expression of this receptor was exclusively detectable in endothelial cells in all tissues examined of *TIE2-tva* transgenic but not wild-type mice (Figure 1A and data not shown). Moreover, all endothelial cells expressing TVA also expressed $\alpha_3\beta_1$ integrin (Figure 1B), the cellular receptor for KSHV (Akula et al., 2002), suggesting that the TVA-expressing cells in the *TIE2-tva* mouse correspond to those naturally targeted by KSHV.

To examine whether TVA-expressing endothelial cells were susceptible to ALV-derived viral infection in vivo, we tested virus expressing the polyoma middle T antigen (PyMT), which induces multifocal hemorrhages and benign endotheliomas when expressed in animals by retroviral transduction (Ong et al., 2001; Williams et al., 1988). PyMT protein could be detected in chicken fibroblasts (DF-1) (Himly et al., 1998; Schaefer-Klein et al., 1998) transfected with the subgroup A avian leukosis virus-derived cloning vector (RCASBP[A]) (Hughes et al., 1987) carrying PyMT (RCAS-*PyMT*) (Figure 2A). Infection with the viral supernatant collected from RCAS-*PyMT* DF-1 producer cells resulted in expression of PyMT in immortalized murine endothelial cells (SVECs) ectopically expressing TVA (EC-TVA) (Figure 2A). As expected, parental SVECs were resistant to viral infection (Figure 2A), confirming the specificity of this method of gene delivery to TVA expressing cells. We next infected litters resulting from the breeding of *TIE2-tva* heterozygous animals to FVB/N mice, 5 days after birth, by intraperitoneal (IP) injection of RCAS-*PyMT* virus (10^7 IU). Surprisingly, 50% of all injected animals died 9–17 days after injection. Genotyping of infected offspring revealed that no animals carrying the *tva* transgene survived (Figure 2B). Conversely, none of the wild-type-littermate controls exhibited any gross alteration or died, even when observed up to 12 months following injection (Figure 2B). Histological inspection of *TIE2-tva* mice sacrificed ten days after infection with RCAS-*PyMT* revealed massive multifocal hemorrhages in all tissues examined (Figure 2C), likely secondary to loss of vascular integrity in association with endothelial hyperproliferation (Williams et al., 1988). This potent biological activity was dose dependent, and as little as 10^3 IU were sufficient to cause the death of 25% of the *TIE2-tva* injected mice (Figure 2B). These animals developed multiple benign hemangiomas composed of well-differentiated endothelial cells (results not shown), further supporting the specificity of the targeted cell type. Tissue examination of littermate controls or *TIE2-tva* mice infected with RCAS-*AP* or RCAS-β-*lactamase vir*us revealed no pathology up to 18 months following infection (results not shown). These results suggested that the *TIE2-tva* mouse represents a suitable animal model to test the ability of transforming sequences to promote hyperproliferation of endothelial cells after retroviral transduction in vivo.

Delivery of KSHV oncogenes to *TIE2-tva* mice

We next set out to determine which KSHV oncogenes could initiate endothelial cell transformation in *TIE2-tva* mice by engineering avian retroviruses carrying putative KSHV latent transforming or survival genes. Latent genes are expressed in almost all spindle cells in late KS lesions, and are therefore predicted to play a critical role in the progression of Kaposi's sarcomagenesis (Jenner and Boshoff, 2002). Indeed, two KSHV latent genes (*vFlip* and *Kaposin*) have been previously reported to harbor transforming potential in vitro (Djerbi et al., 1999; Muralidhar et al., 1998). To determine their capacity to initiate KS tumorigenesis in vivo, we prepared avian retrovirus encoding the latent genes *vCyclin, vFlip*, or *Kaposin*. Additionally, as two other

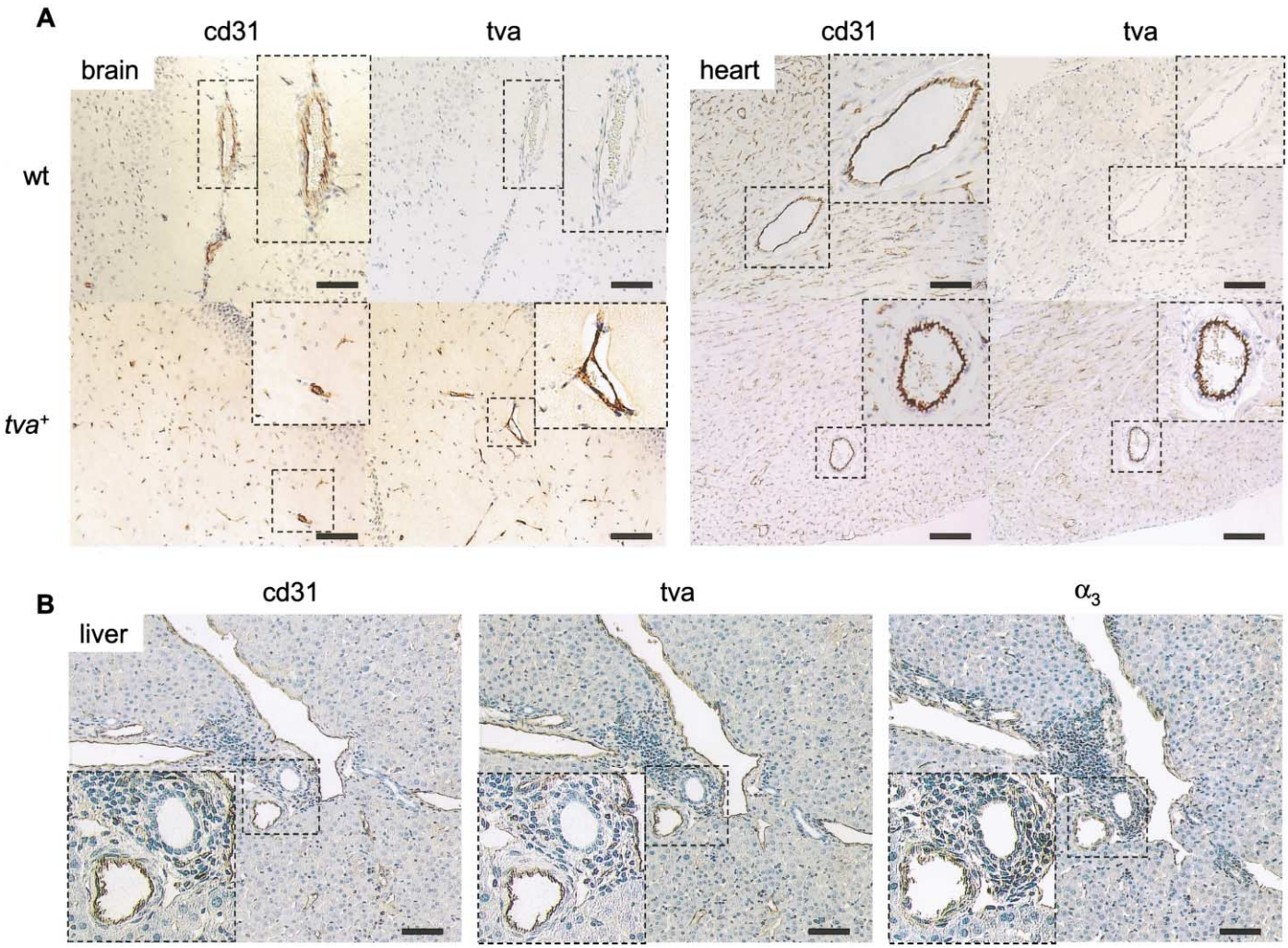

Figure 1. Coexpression of the receptor for the avian leukosis virus, TVA, and the KSHV cellular receptor, $\alpha_3\beta_1$ integrin, in endothelial cells of *TIE2-tva* transgenic mice

A: Immunohistochemical detection of TVA in endothelial cells, using the TVA antibody. Staining of TVA correlates with endothelial-specific staining of blood vessels for CD31 (PECAM-1), in the brain and heart of *TIE2-tva* (*tva*$^+$) mice, but it is absent in control (wt) animals.

B: Immunohistochemical staining of a liver of a *TIE2-tva* mouse with CD31 (PECAM-1), TVA, and α_3 integrin antibodies, respectively. Endothelial cells of *TIE2-tva* mouse, stained with CD31 specific antibody, coexpress both TVA and the cellular receptor for KSHV, $\alpha_3\beta_1$ integrin. Scale bar 100 μm.

KSHV-encoded latent genes, *LANA-1* and *LANA-2* (in addition to three other KSHV encoded genes, *vIRF1*, *K8*, and *ORF50*), have been previously suggested to act by inhibiting the tumor suppressor p53 (Friborg et al., 1999; Rivas et al., 2001), we also generated a retrovirus encoding its potent dominant negative mutant, *p53mutV135A* (Harvey et al., 1995). Prior to introducing these viral constructs into animals, they were first tested in cell culture to ensure the appropriate expression and biological activity of the respective gene products. The corresponding encoded proteins of all ALV-derived viral constructs were readily detected by immunoblotting of DF-1 transfected cells (Figure 3A), and by immunofluorescence in EC-TVA infected cells (Figure 3B). The precise subcellular localization of all proteins (plasma membrane (PyMT), perinuclear (vCyclin and vFlip), Golgi membrane (Kaposin), and cytoplasm and nucleus (p53mutV135A) were also verified by immunofluorescence in EC-TVA cells (Figure 3B) and in transfected 293T cells (results not shown). Moreover, vCyclin induction of H1 phosphorylation (Godden-Kent et al., 1997), vFlip activation of the κB responsive element (Liu et al., 2002), Kaposin activation of MAPK (Kliche et al., 2001), and p53mutV135A inhibition of p53 transcriptional activity (Harvey et al., 1995) were all verified in cultured cells to ensure that all viral constructs encoded biologically active proteins (not shown). Surprisingly, although several of the latent genes were predicted to play an important role in driving Kaposi's sarcomagenesis, when injected in isolation, none affected mouse survival (Figure 3B). Furthermore, mice injected with virus encoding both vCyclin and vFlip, using a bicistronic construct (Low et al., 2001) (Figure 3A), similarly failed to manifest any phenotype up to one year following injection (Figure 3B). These results raised the possibility that the KSHV gene responsible for the initiation of Kaposi's sarcomagenesis may not be a latent gene.

We therefore expanded our study to include additional

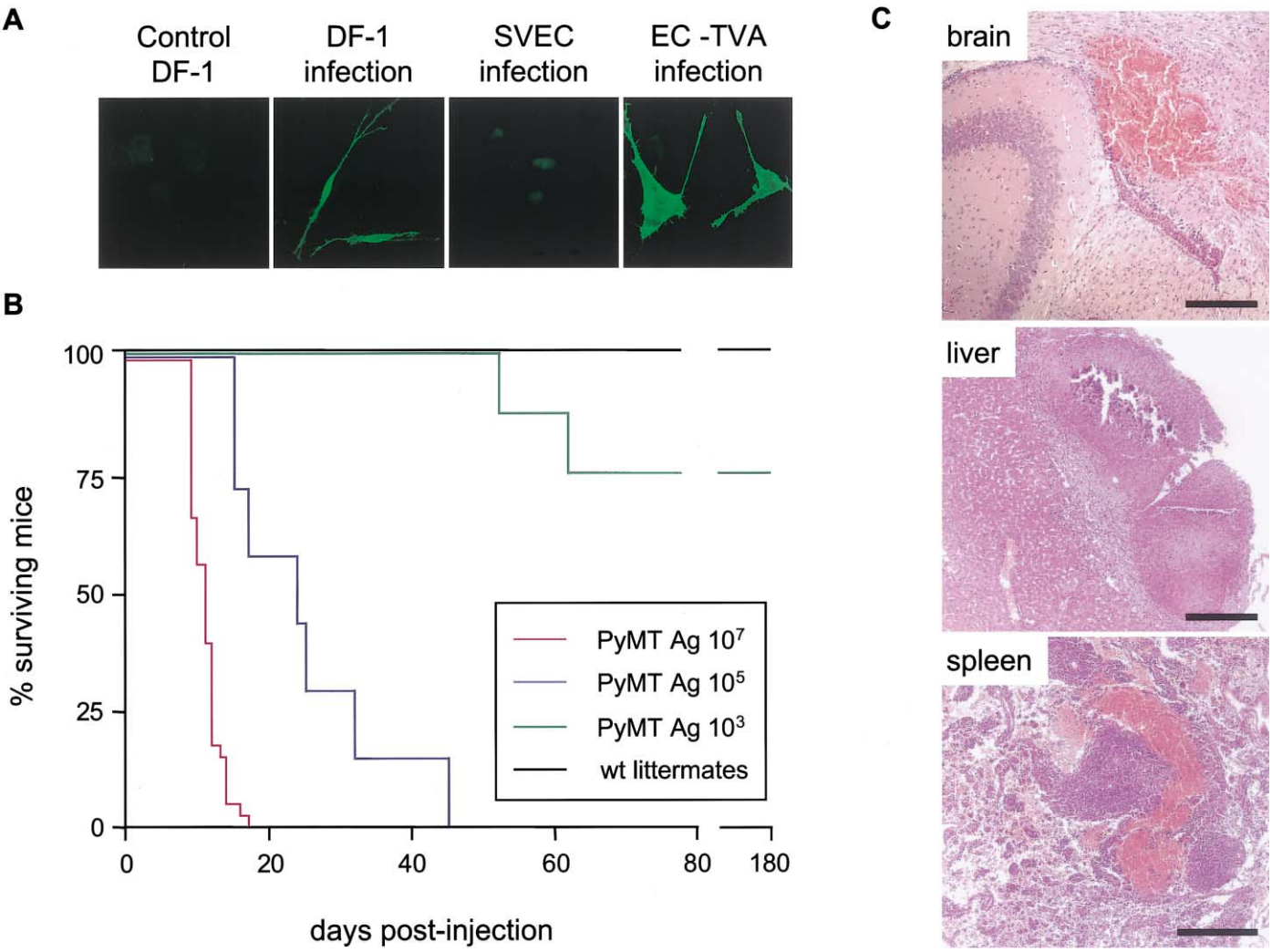

Figure 2. Infection with virus encoding polyoma middle T antigen (PyMT) induces multifocal hemorrhages in *TIE2-tva* mice

A: TVA-expressing cells are permissive to retroviral infection by avian leukosis virus-derived vector (RCAS) encoding PyMT. AU5 tagged PyMT was detected by immunofluorescence in chicken fibroblasts (DF-1), EC-TVA, but not in SVEC after infection with RCAS-*PyMT* virus.

B: Surviving mice (%) after intraperitoneal infection with RCAS-*PyMT* virus. Five-day-old mice born from *TIE2-tva* × FVB/N breeding pairs were injected with the indicated viral loads of RCAS-*PyMT*.

C: Representative H & E stained sections of lesions found in brain, liver, and spleen of *TIE2-tva* mice injected with RCAS-*PyMT* (10^7 IU). All tissues examined showed similar lesions. Scale bar 100 μm.

genes (namely, *vGPCR*, *vIRF-1*, and *vBCL-2*), all also suspected of playing an important role in spindle cell development (Bais et al., 1998; Gao et al., 1997; Sarid et al., 1997). Surprisingly, when injected in isolation, only the retrovirus expressing vGPCR affected mouse survival (Figure 3C). In contrast, necropsies performed six months after infection of *TIE2-tva* mice with the other candidate KSHV oncogenes revealed no gross pathology in multiple independent trials using high viral load (10^7 IU).

vGPCR causes multifocal KS-like tumors

Remarkably, 100% of *TIE2-tva* mice injected with a high viral load (10^7 IU) of RCAS-*vGPCR* virus died within six weeks of infection (Figure 4A). Numerous microscopic tumors compromising the function of multiple organs were observed in these animals (results not shown). In contrast, wild-type littermate controls infected with RCAS-*vGPCR* virus (10^7 IU) were unaffected (Figure 4A).

To determine the contribution of the receptor's constitutive signaling activity observed in vitro (Bais et al., 1998; Montaner et al., 2001) to the phenotype observed in RCAS-*vGPCR*-infected animals in vivo, we prepared an inactive mutant of *vGPCR* containing a 5 amino acid deletion in the carboxyl terminus, *vGPCRΔ5* (Schwarz and Murphy, 2001). Animals infected with high titer virus (10^7 IU) encoding this inactive receptor (RCAS-*vGPCRΔ5*) were not affected and did not present any gross pathology or histopathology when sacrificed up to one year following injection (Figure 4A), suggesting that vGPCR-pathogenesis requires a persistently active receptor.

When infected with virus encoding the constitutively active *vGPCR* (RCAS-*vGPCR*) at a lower viral load (10^5 IU) (Figure 4A),

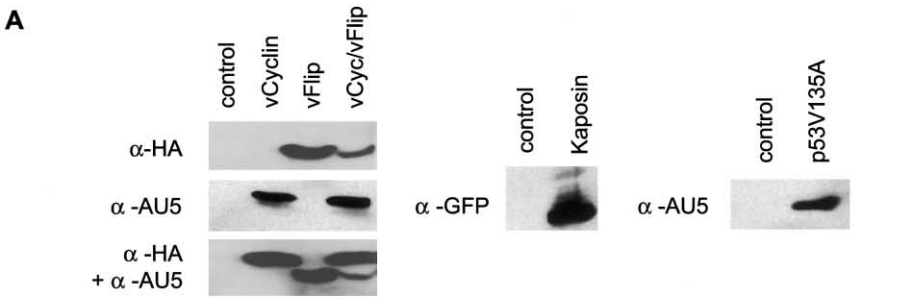

B

EC-TVA infection	Gene	Infective Particles	n^1	Median Survival[2] (up to 180 days) wt	Median Survival[2] (up to 180 days) *tva*$^+$
AU5	*PyMT Ag*	10^7/ml	64	180	10.5[3]
		10^5/ml	13	180	20.5[3]
AU5	*vCyclin*	10^7/ml	22	180	180
HA	*vFlip*	10^7/ml	24	180	180
GFP	*Kaposin*	10^7/ml	15	180	180
AU5	*p53V135A*	10^7/ml	21	180	180
AU5 HA	*vCyc/vFlip*	10^7/ml	29	180	180

C

EC-TVA infection	Gene	Infective Particles	n^1	Median Survival[2] (up to 180 days) wt	Median Survival[2] (up to 180 days) *tva*$^+$
AU5	*vGPCR*	10^7/ml	33	180	38[3]
HA	*vIRF-1*	10^7/ml	14	180	180
AU5	*vBCL-2*	10^7/ml	25	180	180

Figure 3. Median survival of *TIE2-tva* mice following injection with virus expressing candidate KSHV oncogenes

A: Immunoblot of chicken fibroblasts (DF-1) transfected with avian leukosis virus-derived vector (RCAS) encoding candidate latent KSHV oncogenes or the dominant negative p53mutV135A, tagged with HA (vFlip), AU5 (vCyclin and p53mutV135A), or GFP (Kaposin). The bicistronic *vCyc/vFlip* construct is detectable by WB against both AU5 (vCyclin) and HA (vFlip).

B: Infection of *TIE2-tva* mice with latent KSHV oncogenes does not impact mouse survival. Infection of EC-TVA cells in vitro with virus encoding candidate KSHV oncogenes immunodetected using antibody against AU5, HA, or GFP tags (panels on left). Five-day-old mice born from *TIE2-tva* × FVB/N breeding pairs were injected with the indicated viral loads of respective virus.

C: Infection of *TIE2-tva* mice with other KSHV oncogenes. Only injection of *TIE2-tva* mice with virus encoding *vGPCR* affects mouse survival. [1]Total number of animals injected. [2]Median survival of either wt or *tva*$^+$ animals injected. [3]P value $<$ 0.01.

TIE2-tva mice survived longer but developed visible vascular tumors in less than 4 months (Figures 4B and 4C). Necropsy of these mice demonstrated similar lesions involving multiple internal organs (Figures 4D–4H). Histological examination revealed lesions ranging from benign angiectasias and hemangiomas to solid tumors (Figure 5A), the latter composed of whorls of spindle-shaped cells surrounded by abundant blood vessels and erythrocyte-replete vascular slits (Figure 5B). The spindle-shaped tumor cells presented diffuse infiltration of the surrounding normal tissue (Figure 5C). Notably, these cells remained histologically very similar to those of nodular human KS lesions (Figures 5D and 5E). Ultrastructural analysis confirmed that these tumors were highly vascular with tortuous vessels and numerous extravasated erythrocytes (Figure 5F). Like human KS, the aberrant tumor vessels were composed of plump immature endothelial cells with large nuclei encroaching the vessel lumen (Figure 5G). Furthermore, the spindle-shaped tumor cells displayed ovoid, often notched nuclei with finely stippled chromatin, and electron lucent cytoplasm with few organelles, all common features of human KS spindle cells (Bosman et al., 1996) (Figure 5H). Extravasated erythrocytes and occasional erythrophagocytosis, both unique characteristics of human KS lesions, were also observed.

Immunohistochemical analysis revealed that most spindle-shaped tumor cells expressed the endothelial cell markers CD31 and CD34 (Figure 6A), histological hallmarks of KS (Simonart et al., 2000), yet failed to express other endothelial markers, including CD54 (Figure 6A), vWF, and VE-cadherin, as well as

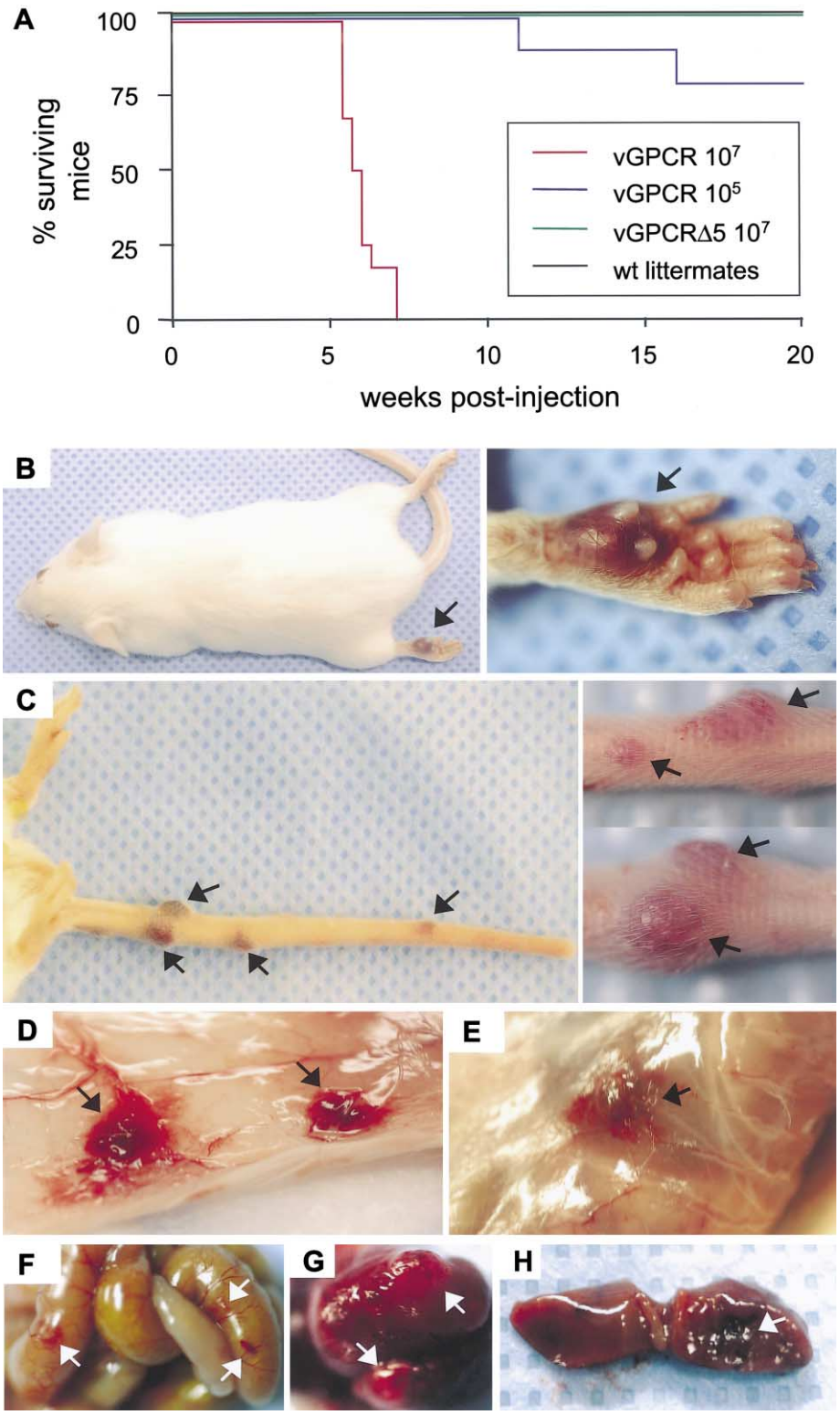

Figure 4. vGPCR induces multifocal angioproliferative tumors in *TIE2-tva* mice

A: Curve shows surviving mice (%) after intraperitoneal injection of the indicated virus into 5-day-old *TIE2-tva* mice and their littermate controls.

B–H: Lesions found in the *TIE2-tva* mice injected with RCAS-*vGPCR* (10^5 IU). Representative vascular tumors found in paw (**B**), tail (**C**), dermis (**D**), peritoneum (**E**), intestine (**F**), heart (**G**), and liver (**H**).

the smooth muscle cell and pericyte marker α-smooth muscle actin (data not shown). Tumor cells were similarly negative for TVA, suggesting loss of *TIE2* promoter activity in these dedifferentiated cells (results not shown). Inflammatory cells were rare within the tumor, despite the presence of frequent peritumoral macrophages (Figure 6B). Interestingly, despite the aggressive nature of these tumors, immunohistochemical and in situ hybridization studies of these lesions revealed that the vGPCR was expressed in only a few tumor cells (Figure 6C), similar to the vGPCR expression pattern seen in human KS lesions (Chiou et

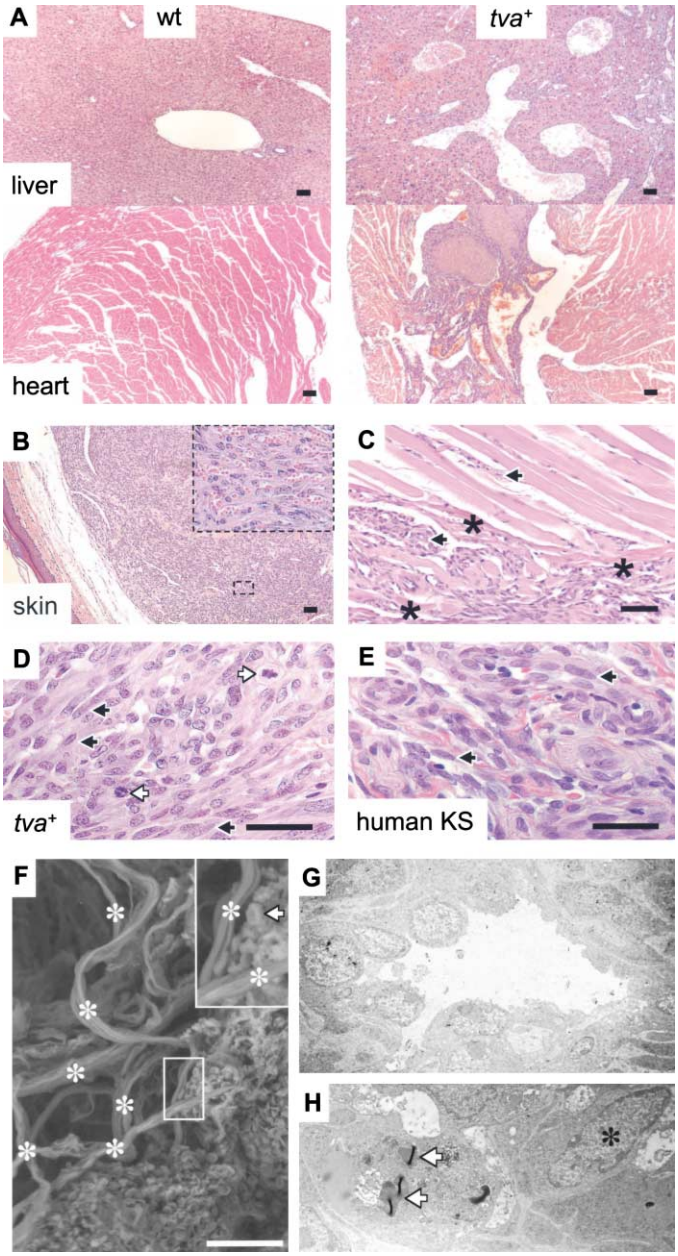

Figure 5. Angioproliferative tumors in vGPCR-injected *TIE2-tva* mice closely resemble human KS lesions

A: Examination of the liver and heart of wt and *TIE2-tva* (*tva*$^+$) animals after injection with RCAS-*vGPCR* (10^5 IU). H & E staining reveals lesions ranging from benign angiectasias (liver) to invasive solid tumors (heart).
B and C: H & E staining of a nodular tumor in the skin. Tumor cells were surrounded by numerous blood vessels and erythrocyte-replete vascular slits (inset) (**B**). **C** shows the presence of spindle-shaped tumor cells (arrows) invading adjacent muscle cells (* = dying muscle cells).
D and E: H & E stained sections of a vGPCR-induced dermal tumor in a *TIE2-tva* mouse and a human KS lesion. Spindle-shaped tumor cells (black arrows) exhibit large nuclei, prominent nucleoli, and occasional mitoses (white arrows) (**D**), which closely resemble spindle cells of human KS lesions (**E**).
F: Scanning electron microscopy of nodular tumor. Tumor vasculature (*) was highly tortuous, with numerous extravasated red blood cells (white arrow).
G and H: Transmission electron microscopy of tumor. Endothelial cells of aberrant tumor vessels were immature, with large nuclei encroaching vessel lumen (**G**). **H** shows typical tumor spindle cell with notched nucleus (*), few organelles, and erythrophagocytosis (white arrows).
A–F: Scale bar 50 μm; **G and H:** original magnification, 3000×.

al., 2002). Staining was performed in both early (6 weeks) and late (20 weeks) tumors with similar results. Thus, the gross, histological, ultrastructural, and immunohistochemical analysis of vGPCR-induced tumors in *TIE2-tva* mice strikingly resembled that of human KS lesions. Taken together, these findings strongly implicate *vGPCR* in the initiation of KS tumor development, and further identify the endothelial cell as the probable cell of origin of the KS spindle cell.

vGPCR promotes the tumorigenic potential of latent KSHV genes through a paracrine mechanism

We next set out to determine the mechanism whereby vGPCR could initiate and promote Kaposi's sarcomagenesis, despite being expressed in only a few tumor cells in both human KS lesions and in our KS animal model. To this end, we prepared endothelial cell lines stably expressing either the vGPCR (EC-vGPCR), the individual KSHV latent genes *vCyclin* or *vFlip* (EC-vCyclin and EC-vFlip, respectively), or both proteins vCyclin and vFlip (EC-vCyc/vFlip) (Low et al., 2001). We took advantage of the SV40 large T antigen immortalized murine endothelial cell line (SVECs), as the large T antigen mimics the inhibition of p53 and Rb by the KSHV latent gene, *LANA-1* (Friborg et al., 1999; Radkov et al., 2000). Expression of the corresponding encoded proteins for all SVEC stable cell lines was readily detected by immunofluorescence (results not shown). When 5×10^5 cells were injected subcutaneously, SVEC cells stably expressing EGFP (EC-EGFP), similar to the parental SVEC cell line, were unable to promote tumor formation in nude mice up to three months following injection (Table 1). EC-vCyclin, EC-vFlip, and the SVEC line stably expressing both latent proteins (EC-vCyc/vFlip) were equally—albeit only weakly—able to promote tumor formation in nude mice six weeks following injection (Table 1). However, EC-vGPCR potently formed tumors in nude mice within two weeks of injection, consistent with our observations of the potency of this oncogene in the *TIE2-tva* model.

Interestingly, similar to studies in the *TIE2-tva* mice, immunohistochemical analysis of the EC-vGPCR tumors revealed that only a few cells within the tumor expressed the oncogene (Figure 7A). *vGPCR* is unique among the putative KSHV oncogenes in that it is both transforming and proangiogenic (Bais et al., 1998). *vGPCR* promotes endothelial cell survival through Akt (Montaner et al., 2001) and induces the transcription of the potent angiogenic polypeptide vascular endothelial growth factor (VEGF) through the activation of HIF-1α (Sodhi et al., 2000, 2001). To assess the involvement of growth factor secretion in vGPCR-mediated Kaposi's sarcomagenesis, we investigated the levels of VEGF in the EC-vGPCR tumors. Immunohistochemical analysis of these lesions revealed that VEGF was prominently expressed in a fraction of tumor cells, an expression pattern similar to what is seen for vGPCR in these lesions (Figure 7A). Moreover, endothelial cells stably expressing the biologically inactive mutant of *vGPCR*, (*vGPCRΔ5*), which does not induce VEGF secretion (results not shown; Schwarz and Murphy, 2001), were unable to form tumors when injected in nude mice (Table 1).

Based on these results, we hypothesized that the ability of vGPCR to form tumors may require the paracrine recruitment and transformation of neighboring cells. To test this hypothesis, nude mice were injected with mixed cell populations in which only a small fraction of cells (10%) were expressing the vGPCR, similar to the expression pattern of this gene in human KS

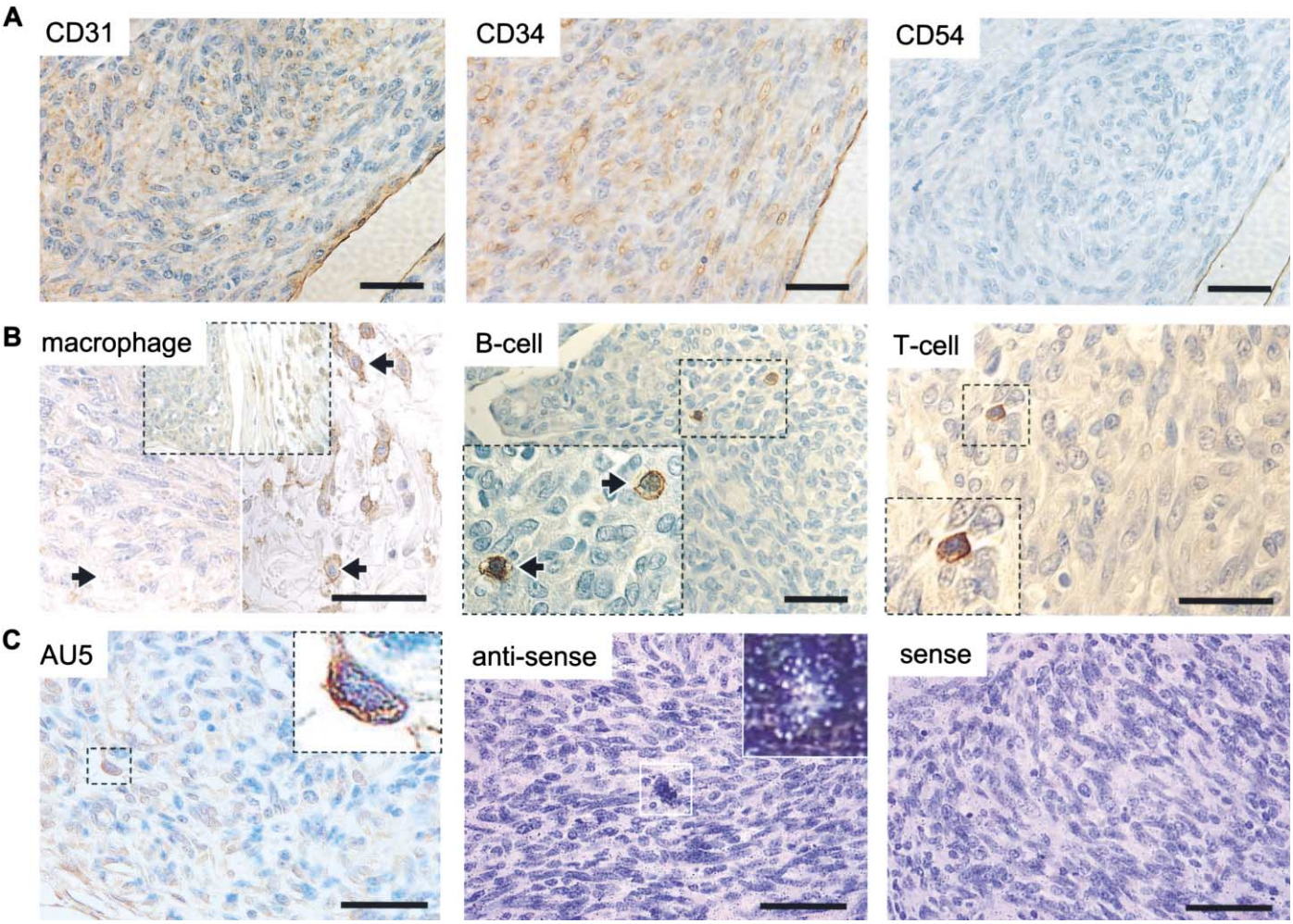

Figure 6. Immunohistochemical characterization of the angioproliferative tumors induced by the vGPCR in *TIE2-tva* mice

A: Staining with CD31 (PECAM-1) and CD34 specific antibodies shows expression both in vascular endothelial cells and tumor cells. CD54 (ICAM-1) was negative in tumor cells.

B: Immunodetection of macrophages (tumor, left; peritumor, right), B cells, and T cells in tumor sections, using F4/80, CD45R/B220, and CD3 antibodies, respectively. Scale bar 50 μm.

C: Representative section stained with anti-AU5 antibody or hybridized to labeled anti-sense probe for *vGPCR* (inset, darkfield) showing expression and transcription of the vGPCR in only few tumor cells.

lesions (Chiou et al., 2002). As shown in Table 1, when a low number of EC-vGPCR (5×10^4 cells) was injected subcutaneously into nude mice, they only rarely (<10% of injected animals) formed small tumors, and only after two months following injection. As mentioned above, injection of a high number of EC-EGFP (5×10^5 cells) alone was unable to form tumors. Surprisingly, injection of a mixed endothelial cell population of both the low amounts of EC-vGPCR (5×10^4 cells) with EC-EGFP (5×10^5 cells) was able to form visible tumors as early as one month following injection in over 50% of injected animals (Table 1), suggesting that vGPCR-expressing endothelial cells are able to rescue the normally nontransforming EC-EGFP cells. Indeed, immunohistochemical analysis of tumors formed by this mixed endothelial cell population revealed a heterogeneous cell population, expressing either the vGPCR or EGFP (Figure 7B).

These observations prompted us to examine whether the latent KSHV genes, which are expressed by the majority of KSHV-infected KS tumor cells (90%) but are not tumorigenic in the *TIE2-tva* mouse model or when expressed in SVEC cells, may however manifest their transforming potential in the context of the paracrine secretions of vGPCR-expressing cells. As an approach, we next injected a low number of EC-vGPCR (5×10^4 cells) mixed with EC-vFLIP or EC-vCyclin (5×10^5) cells. Both EC-vFlip and EC-vCyclin were able to form visible tumors within one month when injected with EC-vGPCR, similar to that observed when the EC-vGPCR cells were mixed with EC-EGFP cells. However, injection of EC-vCyc/vFlip cells (5×10^5 cells) with EC-vGPCR cells (5×10^4 cells) formed tumors in 100% of the animals within only two weeks of injection (Table 1). Of note, these tumors were much larger and grew more rapidly than those formed by the mixed populations of the EC-vGPCR with endothelial cells stably expressing vFlip or vCyclin alone. To confirm the contribution of EC-vCyc/vFlip cells to these lesions, we also examined expression of the HA-tagged vFlip protein in

Table 1. Tumorigenesis of SVEC stable cell lines

SVEC line	Number of cells	n[1]	Tumors[2]
EC-EGFP	5×10^5	20	−
EC-vGPCR	5×10^5	20	+++++
EC-vGPCRΔ5	5×10^5	20	−
EC-vCyclin	5×10^5	10	+
EC-vFlip	5×10^5	10	+
EC-vCyc/vFlip	5×10^5	10	+
EC-vGPCR	5×10^4	10	+/−
EC-vGPCR + EC-EGFP	5×10^4		
	5×10^5	10	++
EC-vGPCR + EC-vCyclin	5×10^4		
	5×10^5	10	+++
EC-vGPCR + EC-vFlip	5×10^4		
	5×10^5	10	+++
EC-vGPCR + EC-vCyc/vFlip	5×10^4		
	5×10^5	10	+++++
EC-vGPCRΔ5 + EC-vCyc/vFlip	5×10^4		
	5×10^5	10	+

6-week-old female Nu/Nu mice were injected subcutaneously (SQ) with SVECs stably expressing candidate KSHV oncogenes.
[1]Total number of animals injected.
[2]Tumor formation 6 weeks following injection; tumorigenic potential was quantitated as follows: no tumors (−); tumors in less than 25% of mice injected, <25 mg (+); tumors in 25%–75% of mice injected, 25–50 mg (++); tumors in 75%–100% of mice injected, 50–100 mg (+++); tumors in 75%–100% of mice injected, 100–150 mg (++++); tumors in 75%–100% of mice injected, >150 mg (+++++).

EC-vGPCR + EC-vCyc/vFlip mixed cell tumors. Immunohistochemical analysis revealed that most cells were indeed derived from the EC-vCyc/vFlip cell line (Figure 7C), an expression pattern similar to what is seen in human KS lesions (Gruffat et al., 2000).

In addition to its role in the initiation of KS tumors, these results strongly suggest that the vGPCR may also participate in KS tumor progression by unmasking the tumorigenic potential of latent KSHV genes. Investigation of VEGF levels in the EC-vGPCR + EC-vCyc/vFlip mixed cell tumors revealed that VEGF was again only expressed in a fraction of tumor cells (Figure 7C). Conversely, endothelial cells stably expressing the biologically inactive mutant of *vGPCR, vGPCRΔ5*, were not tumorigenic and did not promote tumor formation when injected at low concentration (5×10^4 cells) together with EC-vCyc/vFlip (5×10^5 cells) (Table 1), suggestive of a requirement for constitutive activity for vGPCR pathogenesis. Collectively, these results strongly suggest that vGPCR recruits and transforms latently infected endothelial cells through a paracrine mechanism involving the secretion of angiogenic growth factors, such as VEGF, and further identify this viral oncogene as a key target for the development of pathogenesis-based therapies against KSHV.

Discussion

We engineered transgenic animals expressing the avian retroviral receptor, TVA, under the *TIE2* promoter, to enable endothelial cell-specific infection with avian leukosis virus expressing KSHV genes believed to play a role in spindle cell growth and survival. *TIE2-tva* mice infected with the KSHV gene, *vGPCR*, developed vascular tumors that closely resembled human KS lesions and expressed key histopathological and molecular hallmarks for this disease. Spindle-shaped tumor cells were dedifferentiated, yet retained expression of several, but not all, endothelial markers, similar to human KS lesions (Simonart et al., 2000). In addition to their remarkable histological and ultrastructural similarity to human KS lesions, vGPCR-induced tumors had a unique predilection for the dermis, similar to human KS. This is in striking contrast to other oncogenes introduced into *TIE2-tva* mice (e.g., polyoma middle T antigen), which did not form visible skin lesions in multiple independent trials, despite a potent ability to form endothelial tumors in almost all other tissues examined (results not shown). These results suggest that dermal endothelial cells may be particularly vulnerable to vGPCR-induced Kaposi's sarcomagenesis, perhaps explaining why systemic infection with KSHV often manifests only with dermal KS lesions. This compelling congruence between vGPCR-induced tumors and human Kaposi's sarcoma suggests the importance of exploring *vGPCR* oncogenesis to fully understand KSHV pathogenesis.

Of note, expression of the vGPCR in T-cells has been shown to produce tumors in transgenic mice (Yang et al., 2000). However, this observed phenotype may have resulted from the accumulation of genetic changes induced by the persistent expression of the vGPCR in lymphoid cells during development, a process unlikely to play a role in Kaposi's sarcomagenesis. The *TIE2-tva* model may reflect better the function of this receptor in KS, as it recreates more faithfully the in vivo infectious process by which KSHV infects a limited number of cells of endothelial origin (Flore et al., 1998).

Indeed, in our model, similar to human KS, few of these tumor cells expressed the vGPCR (Chiou et al., 2002). This suggests that receptor expression may be lost once the cells are transformed and the receptor is no longer needed for cell survival. However, we cannot rule out the possibility that expression of this GPCR in our KS model—and in human KS—may be at such low levels that its detection may be limited by the inherent sensitivity of the techniques used. Alternatively, vGPCR-expressing cells may promote the recruitment, hyperproliferation, and subsequent transformation of adjacent cells through the secretion of multiple cytokines and potent polypeptide growth factors (Bais et al., 1998; Couty et al., 2001; Pati et al., 2001; Schwarz and Murphy, 2001; Sodhi et al., 2000). The ability of the receptor to cause endothelial cell survival in vitro (Montaner et al., 2001) and the release of growth factors and cytokines from vGPCR-expressing cells (Bais et al., 1998; Pati et al., 2001; Schwarz and Murphy, 2001; Sodhi et al., 2000) argue in favor of a role for *vGPCR* in both direct transformation and in paracrine recruitment. Indeed, cells expressing the *vGPCR* express elevated levels of the angiogenic growth factors including VEGF (results not shown, Bais et al., 1998). Furthermore, media conditioned by vGPCR-expressing cells promotes the growth and proliferation of endothelial cells (results not shown; Bais et al., 1998). We also show here that endothelial cells stably expressing vGPCR can unmask the tumorigenic potential of KSHV latent genes, suggestive of a cooperative role between *vGPCR* and viral latent genes in KS tumor progression.

In the context of the *TIE2-tva* model, none of the other KSHV genes tested was able to cause a biological effect, in spite of evidence that several of them can transform cell lines in vitro. The corresponding encoded proteins of all ALV-derived viral constructs were readily detected by immunodetection in murine endothelial cells (ectopically expressing TVA) infected in vitro. However, due to the limited number of endothelial cells infected

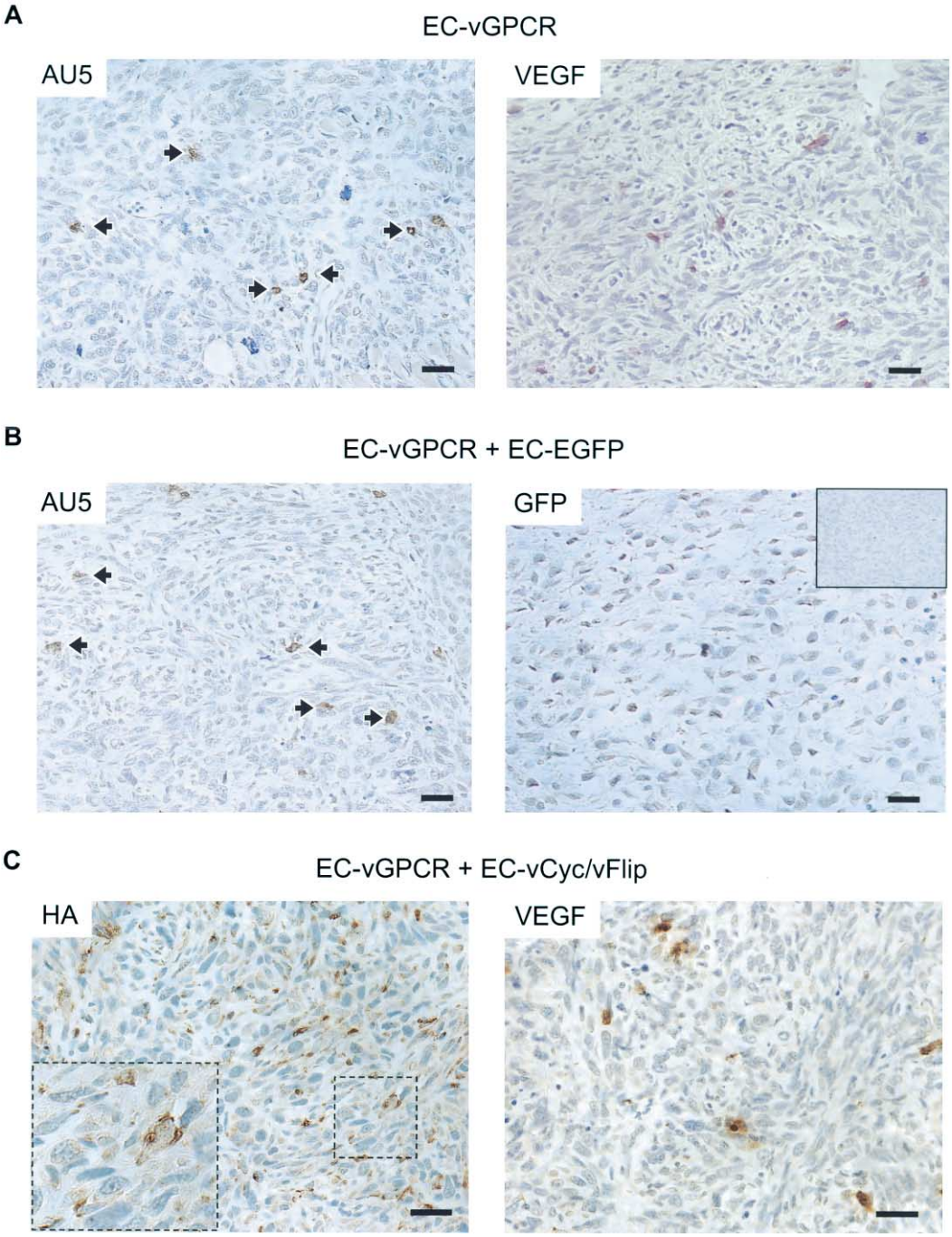

Figure 7. Immunohistochemical characterization of the allograft tumors formed by mixed population of SVEC stable cell lines in nude mice

A: Left, representative section of tumor formed by 5×10^5 EC-vGPCR cells stained with anti-AU5 antibody showing rare vGPCR-expressing cells (black arrows). Right, EC-vGPCR tumor stained with anti-VEGF antibody showing expression of VEGF in few tumor cells, an expression pattern similar to that seen for vGPCR-expressing cells.

B: Left, tumor formed by mixed cell population of 5×10^4 EC-vGPCR with 5×10^5 EC-EGFP stained with anti-AU5 antibody showing rare vGPCR-expressing cells (black arrows). Right, staining with EGFP specific antibody shows expression of GFP in many tumor cells. Inset, EGFP expression in EC-vGPCR tumors (**A**) was negative.

C: Left, representative section of tumor formed by mixed cell population of 5×10^4 EC-vGPCR mixed with 5×10^5 EC-vCyc/vFlip stained with anti-HA antibody showing characteristic punctate expression of HA-vFlip in most tumor cells. Right, tumor formed by EC-vGPCR + EC-vCyc/vFlip stained with anti-VEGF antibody showing expression of VEGF in few tumor cells, an expression pattern similar to that seen in **A** in EC-vGPCR tumors. Scale bar 50 μm.

in *TIE2-tva* mice, we could not confirm the expression of the latent genes in vivo. Consequently, we cannot rule out the possibility that the level of gene expression in the *TIE2-tva* model was insufficient for the animals to manifest an overt phenotype. Nonetheless, these results suggest that infection of endothelial cells with individual KSHV latent genes alone may not be sufficient for transformation in vivo. Rather, these genes may cooperate with the vGPCR and with each other, or may further require HIV-1 genes (e.g., *tat*) (Barillari and Ensoli, 2002) in the context of an immunosuppressed host to exhibit their transforming potential. Since multiple genes may be delivered to the same endothelial cells of *TIE2-tva* mice, this mouse model will be ideally suited to address this complex interplay among KSHV genes, as well as the contribution of HIV-1 and immunosuppression to KSHV oncogenesis.

The vGPCR has been designated as a lytic gene based on in vitro experiments using chemicals to induce expression from virally infected B cells from a primary effusion lymphoma (PEL) cell line (Sun et al., 1999). However, these studies may not define the events that occur early in the in vivo infectious process, and may not be predictive of the ability of these viral genes to initiate host cell transformation. Moreover, as few individuals infected by KSHV go on to manifest Kaposi's sarcoma, it is likely that deregulation of normal viral gene expression programs may play a fundamental role in the development of this disease. Thus, KSHV genes that are not normally expressed during the latent cycle may still play an important role in the initiation of Kaposi's sarcoma. In this regard, recent findings suggest that infection with HIV-1 upregulates expression of KSHV lytic genes (Varthakavi et al., 2002). Within this framework, we envision that the viral GPCR may serve as a transforming gene upon deregulated expression, as occurs with HIV infection. Indeed, AIDS-KS lesions show increased expression of vGPCR and are significantly more aggressive than classic KS lesions (Yen-Moore et al., 2000).

Alternatively, the vGPCR may initiate cell transformation when expressed transiently, early in the infectious process. The expression of this receptor may then create an environment in which subsequent tumor development can occur in the presence of other KSHV survival genes, after which receptor expression may become unnecessary (Cesarman et al., 2000). This "hit-and-run" mechanism is certainly not without precedent. It has been extensively documented for the major transforming protein of the human T cell leukemia virus-1 (HTLV-1), Tax, which is only expressed in early stages of tumor formation and is not required in established T cell malignancies (Yoshida, 2001). Similarly, papilloma virus E5 also appears to play a critical role in cell transformation early in infection, and yet is rarely detected once tumors are formed (DiMaio and Mattoon, 2001). For the vGPCR, expression of the receptor during the viral lytic cycle may also be important in sustaining tumor growth through a paracrine mechanism, as supported by our results demonstrating that the vGPCR can unmask the tumorigenic potential of latent KSHV genes through the secretion of angiogenic growth factors including VEGF. This is further supported by recent evidence demonstrating that interruption of lytic replication can impair KS tumor development at all stages of the natural history of KSHV infection (Martin et al., 1999).

Taken together, these data and our present findings strongly suggest that the vGPCR is likely to play a critical role in both the initiation and promotion of KS tumor development. Of interest, in vitro data on the vGPCR has revealed that this receptor signals through multiple intracellular regulatory pathways (Bais et al., 1998; Couty et al., 2001; Montaner et al., 2001; Pati et al., 2001; Sodhi et al., 2000). As GPCRs have proven to be effective targets for pharmacological intervention (Marinissen and Gutkind, 2001), our findings thus suggest that the vGPCR and its downstream signaling routes may represent ideal targets for the development of pathogenesis-based therapies against KSHV. In this regard, our animal model may now help elucidate the biological significance of the intervening signaling molecules in the development of KS and may further identify effective treatments for this elusive disease. Ultimately, the *TIE2-tva* model may be similarly exploited in the context of many other diseases that are also known to involve the aberrant function of endothelial cells, as it enables examination of the biological outcome of expressing specific genes of interest in endothelial cells in vivo, using a single transgenic animal.

Experimental procedures

Mouse strains

The *TIE2-tva* transgene was generated by insertion of the pg800 *tva* cDNA (Bates et al., 1993; Young et al., 1993) as a NotI fragment into a bluescript SK (+) vector containing the murine 2.1 kb HindIII *TIE2* promoter fragment and SV40 poly (A) signal sequence. The plasmid also included, downstream of the *tva* cassette, a 10 kb autonomous endothelial-specific enhancer located in the first intron of the mouse *TIE2* gene, which allows specific and uniform gene expression to all vascular ECs in vivo (Schlaeger et al., 1997). The *TIE2-tva* insert was isolated after digestion by SalI. Transgenic mice were generated in FVB/N mice using standard techniques and identified by Southern blot using the *tva* cDNA as a probe. Genotypes were determined by Southern blotting and by PCR with tail DNA. The athymic (*nu/nu*) nude females were purchased from Harlan Sprague Dawley.

Viral constructs

The KHSV genome was obtained from NIH AIDS Research & Reference Reagent Program and open reading frames encoding for *v-Cyclin* (ORF72), *Kaposin* (K12), *vIRF1* (K9), *vFLIP* (ORF71), *vBcl2* (ORF 16), *vGPCR* (ORF74), and both *v-Cyclin* and *vFlip* (bicistronic construct) were cloned by PCR based on their published sequences (Low et al., 2001; Russo et al., 1996). The vGPCRΔ5 mutant (deletion of carboxyl terminal amino acids 338 to 342) was obtained by PCR using a 3′ oligo encoding amino acids 332 to 337 followed by a stop codon and a Not I site. The dominant negative p53 mutant V135A was obtained from Clontech. cDNA encoding for an intracellular form of the β-lactamase enzyme was obtained by PCR using pGEX 4T-3 as a template. To prepare the viral constructs, cDNAs were subcloned into pCEFL-HA, pCEFL-AU5, or pCEFL-EGFP to generate epitope-tagged forms of these gene products, and then transferred into the RCAS vector. The polyomavirus middle T antigen from RCAS-*PyMT* (Holland et al., 2000) was tagged by cloning into pCEFL-AU5, and then subcloned again into RCAS. RCAS-*AP*, encoding the heat-resistant placental alkaline phosphatase has been previously described (Federspiel et al., 1994).

Cell lines and transfections

SV-40 immortalized murine endothelial cells (SVECs) were grown in Dulbecco's modified Eagle's medium (DMEM) supplemented with 10% fetal bovine serum (FBS) and 1% penicillin/streptomycin. Transfection of SVECs was performed using Fugene Reagent (Roche Applied Science). SVEC cells expressing TVA, EGFP, or KSHV genes were obtained by stable transfection of the corresponding pCEFL-derived plasmids (EC-lines). DF-1 chicken fibroblasts were maintained in DMEM with high glucose, supplemented with 10% FBS and 1% penicillin/streptomycin. DF-1 cells were transfected using Superfect reagent (Qiagen).

Preparation of virus and infection of transgenic mice

DF-1 cells were transfected with RCAS vectors to produce recombinant viruses. After several days of passage in culture, cell-free viral supernatants were ultracentrifuged in an SW28 Beckman rotor at 22,000 rpm at 4°C for

two hours. Pellets were resuspended in 1/100 of the original volume and viral titers were determined by limiting dilution. Briefly, EC-TVA cells were seeded into 6-well culture dishes at 30% confluence and infected with serial 10-fold dilutions of concentrated viral supernatants in growth medium. The number of cells expressing the retroviral-transduced proteins was determined by immunofluorescence, and viral titer was expressed as number of infective units (IU) per ml. Viral stocks were injected intraperitoneally into 5-day-old littermates (100 μl/mouse) at the indicated viral load. Mice were genotyped at 21 days of age.

Establishment of tumor allografts in athymic (*nu/nu*) nude mice

SVEC stable cell lines (EC-lines) were used to induce allografts in 5–6 weeks athymic (*nu/nu*) nude females. Exponentially growing cells were harvested, washed with PBS, and resuspended in DMEM, and 5×10^5 viable cells were transplanted subcutaneously in the right flank of the mouse (ten mice per group). For the mixed cell populations, 5×10^4 EC-vGPCR or EC-vGPCRΔ5 cells were combined with 5×10^5 SVEC cells (from the specified cell line) prior to injection. The animals were monitored three times weekly for tumor formation for three months. For analysis, tumor weight was determined by converting tumor volume ($LW^2/2$) (where L and W represent longest length and shortest width of the tumor) to weight.

Fluorescence microscopy and immunohistochemistry

Cells were grown in 24-well plates on coverslips and infected with the corresponding concentrated virus. Thirty-six hours later, cells were fixed and permeabilized with 4% paraformaldehyde and 0.05% Triton X-100 in 1× PBS for 10 min. Coverslips were blocked with 1% BSA and incubated with primary antibodies against epitope tags (Covance) for 1 hr and with secondary antibody conjugated to fluorescein isothiocyanate (Jackson ImmunoResearch Laboratories, Inc.) for 30 min. Coverslips were mounted and visualized using Axioplan2 microscope (Zeiss). For immunohistochemical staining, tissues were fixed in 4% paraformaldehyde, 1 × PBS for 36 hr, transferred to 70% ethanol/PBS, and embedded in paraffin. Sections were cleared in a graded xylene/ethanol series and treated with 3% hydrogen peroxide/H_2O for 20 min. Antigens were retrieved and sections were blocked with 2% equine serum in PBS for 20 min and incubated with the primary antibody at 4°C overnight. After successive incubations with the corresponding biotinylated IgG (Vector Laboratories) and the ABC solution (Vectastain Elite kit, Vector Laboratories), the peroxidase activity was developed using 3-3′ diaminobenzidine as a substrate. Slides were counterstained with hematoxylin, dehydrated, and mounted with Permount (Fisher Scientific). Affinity-purified rabbit polyclonal anti-TVA antibody (Bates et al., 1993) was obtained from Andrew Leavitt (UCSF). Mouse anti-AU5 monoclonal antibody was obtained from Covance. Rat anti-mouse monoclonal antibodies against CD31 (PECAM-1) or CD34 as well as biotinylated rat anti-mouse CD45R/B220 were obtained from Pharmingen. T lymphocytes and macrophages were detected with rabbit anti-human CD3 antibody (DAKO) or rat anti-mouse F4/80 antibody (Caltag Laboratories), respectively. Rat anti-mouse CD54 (ICAM-1) monoclonal antibody and rabbit anti-human α_3 integrin polyclonal antibody were obtained from Chemicon International. Rabbit polyclonal anti-green fluorescent protein (GFP) antibody was purchased from Molecular Probes. Rabbit polyclonal anti-HA and anti-VEGF antibodies were obtained from Santa Cruz Biotechnology.

In situ hybridization

Antisense and sense riboprobes for *vGPCR* were prepared and in situ hybridization on paraffin-embedded tumor sections was performed as previously described (Engelholm et al., 2001). Sections were counterstained with hematoxylin and eosin, mounted in Pertex (Prohospital), and photographed with a Photometrics Coolsnap CCD camera (Rober Scientific) mounted on a transmission microscope (Leitz).

Electron microscopy

Tissues were fixed in 4% formaldehyde/4% glutaraldehyde in 0.1 M cacodylate buffer (pH 7.4) for 3 days, rinsed in cacodylate buffer and incubated overnight in 2% glycine, overnight in 2% tannic acid (pH 4.0), and 6 hr in 2% OsO_4. For scanning EM, the fixed tissues were dehydrated in graded ethanol solutions, put under vacuum for 2 hr, and mounted onto stubs with Leit-C adhesive (Electron Microscopy Sciences). Scanning electron microscopy (SEM) was performed using a Hitachi S-3500N variable pressure scanning electron microscope equipped with a PGT-IMIX-PC EDS system. Transmission electron microscopy (TEM) was performed by using a JEOL 100-CXII.

Acknowledgments

We thank Harold E. Varmus (MSKCC) for insightful suggestions and discussion, Thomas N. Sato (University of Texas) for providing the plasmid containing the *TIE2* promoter-enhancer, Steve Hughes (FCRC, NCI, NIH) for the RCAS and RCAS-*AP* plasmids, Doug Foster (University of Minnesota) for the DF-1 cell line, Andrew Leavitt (UCSF) for the TVA antibody, the Gene Targeting Core Facility (NIDCR) for technical assistance with the development of the transgenic line, Martin Kriete and the Veterinary Resources Core Facility (NIDCR) for assistance with the animal care, SAIC Frederick for tissue preparation and immunohistochemical staining, Keith Rogers for technical assistance, Miriam Anvers for assistance with the histological analysis of pathology samples, and William D. Swaim for assistance with the electron microscopy. This work has been supported by NIH grants 2RO-1 DK 49419, 2RO-1 HL 55605 (PER), and RO-1 AI46145-01A2 and a grant from the Department of Defense, BC972195.

Received: September 20, 2002
Revised: November 22, 2002
Published online: December 20, 2002
DOI: 10.1016/S1535610802002374

References

Akula, S.M., Pramod, N.P., Wang, F.Z., and Chandran, B. (2002). Integrin α3β1 (CD 49c/29) is a cellular receptor for Kaposi's sarcoma-associated herpesvirus (KSHV/HHV-8) entry into the target cells. Cell *108*, 407–419.

Bais, C., Santomasso, B., Coso, O., Arvanitakis, L., Raaka, E.G., Gutkind, J.S., Asch, A.S., Cesarman, E., Gershengorn, M.C., Mesri, E.A., and Gerhengorn, M.C. (1998). G-protein-coupled receptor of Kaposi's sarcoma-associated herpesvirus is a viral oncogene and angiogenesis activator. Nature *391*, 86–89.

Barillari, G., and Ensoli, B. (2002). Angiogenic effects of extracellular Human Immunodeficiency Virus Type 1 tat protein and its role in the pathogenesis of AIDS-associated Kaposi's sarcoma. Clin. Microbiol. Rev. *15*, 310–326.

Bates, P., Young, J.A., and Varmus, H.E. (1993). A receptor for subgroup A Rous sarcoma virus is related to the low density lipoprotein receptor. Cell *74*, 1043–1051.

Boshoff, C., and Chang, Y. (2001). Kaposi's sarcoma-associated herpesvirus: a new DNA tumor virus. Annu. Rev. Med. *52*, 453–470.

Bosman, C., Bisceglia, M., and Quirke, P. (1996). Ultrastructural study of Kaposi's sarcoma. Pathologica *88*, 8–17.

Cesarman, E., Mesri, E.A., and Gershengorn, M.C. (2000). Viral G protein-coupled receptor and Kaposi's sarcoma: a model of paracrine neoplasia? J. Exp. Med. *191*, 417–422.

Chang, Y., Cesarman, E., Pessin, M.S., Lee, F., Culpepper, J., Knowles, D.M., and Moore, P.S. (1994). Identification of herpesvirus-like DNA sequences in AIDS-associated Kaposi's sarcoma. Science *266*, 1865–1869.

Chiou, C.J., Poole, L.J., Kim, P.S., Ciufo, D.M., Cannon, J.S., ap Rhys, C.M., Alcendor, D.J., Zong, J.C., Ambinder, R.F., and Hayward, G.S. (2002). Patterns of gene expression and a transactivation function exhibited by the vGCR (ORF74) chemokine receptor protein of Kaposi's sarcoma-associated herpesvirus. J. Virol. *76*, 3421–3439.

Couty, J.P., Geras-Raaka, E., Weksler, B.B., and Gershengorn, M.C. (2001). Kaposi's sarcoma-associated herpesvirus G protein-coupled receptor signals through multiple pathways in endothelial cells. J. Biol. Chem. *276*, 33805–33811.

DiMaio, D., and Mattoon, D. (2001). Mechanisms of cell transformation by papillomavirus E5 proteins. Oncogene *20*, 7866–7873.

Djerbi, M., Screpanti, V., Catrina, A.I., Bogen, B., Biberfeld, P., and Grandien, A. (1999). The inhibitor of death receptor signaling, FLICE-inhibitory protein defines a new class of tumor progression factors. J. Exp. Med. *190*, 1025–1032.

Dupin, N., Fisher, C., Kellam, P., Ariad, S., Tulliez, M., Franck, N., van Marck, E., Salmon, D., Gorin, I., Escande, J.P., et al. (1999). Distribution of human herpesvirus-8 latently infected cells in Kaposi's sarcoma, multicentric Castleman's disease, and primary effusion lymphoma. Proc. Natl. Acad. Sci. USA *96*, 4546–4551.

Engelholm, L.H., Nielsen, B.S., Netzel-Arnett, S., Solberg, H., Chen, X.D., Lopez Garcia, J.M., Lopez-Otin, C., Young, M.F., Birkedal-Hansen, H., Dano, K., et al. (2001). The urokinase plasminogen activator receptor-associated protein/endo180 is coexpressed with its interaction partners urokinase plasminogen activator receptor and matrix metalloprotease-13 during osteogenesis. Lab. Invest. *81*, 1403–1414.

Federspiel, M.J., Bates, P., Young, J.A., Varmus, H.E., and Hughes, S.H. (1994). A system for tissue-specific gene targeting: transgenic mice susceptible to subgroup A avian leukosis virus-based retroviral vectors. Proc. Natl. Acad. Sci. USA *91*, 11241–11245.

Fisher, G.H., Orsulic, S., Holland, E., Hively, W.P., Li, Y., Lewis, B.C., Williams, B.O., and Varmus, H.E. (1999). Development of a flexible and specific gene delivery system for production of murine tumor models. Oncogene *18*, 5253–5260.

Flore, O., Rafii, S., Ely, S., O'Leary, J.J., Hyjek, E.M., and Cesarman, E. (1998). Transformation of primary human endothelial cells by Kaposi's sarcoma-associated herpesvirus. Nature *394*, 588–592.

Friborg, J., Jr., Kong, W., Hottiger, M.O., and Nabel, G.J. (1999). p53 inhibition by the LANA protein of KSHV protects against cell death. Nature *402*, 889–894.

Ganem, D. (1997). KSHV and Kaposi's sarcoma: the end of the beginning? Cell *91*, 157–160.

Gao, S.J., Boshoff, C., Jayachandra, S., Weiss, R.A., Chang, Y., and Moore, P.S. (1997). KSHV ORF K9 (vIRF) is an oncogene which inhibits the interferon signaling pathway. Oncogene *15*, 1979–1985.

Godden-Kent, D., Talbot, S.J., Boshoff, C., Chang, Y., Moore, P., Weiss, R.A., and Mittnacht, S. (1997). The cyclin encoded by Kaposi's sarcoma-associated herpesvirus stimulates cdk6 to phosphorylate the retinoblastoma protein and histone H1. J. Virol. *71*, 4193–4198.

Gruffat, H., Sergeant, A., and Manet, E. (2000). Kaposi's sarcoma-associated herpesvirus and Kaposi's sarcoma. Microbes Infect. *2*, 671–680.

Harvey, M., Vogel, H., Morris, D., Bradley, A., Bernstein, A., and Donehower, L.A. (1995). A mutant p53 transgene accelerates tumour development in heterozygous but not nullizygous p53-deficient mice. Nat. Genet. *9*, 305–311.

Hermans, P. (2000). Kaposi's sarcoma in HIV-infected patients: treatment options. HIV Med *1*, 137–142.

Himly, M., Foster, D.N., Bottoli, I., Iacovoni, J.S., and Vogt, P.K. (1998). The DF-1 chicken fibroblast cell line: transformation induced by diverse oncogenes and cell death resulting from infection by avian leukosis viruses. Virology *248*, 295–304.

Holland, E.C., Li, Y., Celestino, J., Dai, C., Schaefer, L., Sawaya, R.A., and Fuller, G.N. (2000). Astrocytes give rise to oligodendrogliomas and astrocytomas after gene transfer of polyoma virus middle T antigen in vivo. Am. J. Pathol. *157*, 1031–1037.

Hughes, S.H., Greenhouse, J.J., Petropoulos, C.J., and Sutrave, P. (1987). Adaptor plasmids simplify the insertion of foreign DNA into helper-independent retroviral vectors. J. Virol. *61*, 3004–3012.

Jenner, R.G., and Boshoff, C. (2002). The molecular pathology of Kaposi's sarcoma-associated herpesvirus. Biochim. Biophys. Acta *1602*, 1–22.

Kliche, S., Nagel, W., Kremmer, E., Atzler, C., Ege, A., Knorr, T., Koszinowski, U., Kolanus, W., and Haas, J. (2001). Signaling by human herpesvirus 8 kaposin A through direct membrane recruitment of cytohesin-1. Mol. Cell *7*, 833–843.

Liu, L., Eby, M.T., Rathore, N., Sinha, S.K., Kumar, A., and Chaudhary, P.M. (2002). The human herpes virus 8-encoded viral FLICE inhibitory protein physically associates with and persistently activates the IκB kinase complex. J. Biol. Chem. *277*, 13745–13751.

Low, W., Harries, M., Ye, H., Du, M.Q., Boshoff, C., and Collins, M. (2001). Internal ribosome entry site regulates translation of Kaposi's sarcoma-associated herpesvirus FLICE inhibitory protein. J. Virol. *75*, 2938–2945.

Marinissen, M.J., and Gutkind, J.S. (2001). G-protein-coupled receptors and signaling networks: emerging paradigms. Trends Pharmacol. Sci. *22*, 368–376.

Martin, D.F., Kuppermann, B.D., Wolitz, R.A., Palestine, A.G., Li, H., and Robinson, C.A. (1999). Oral ganciclovir for patients with cytomegalovirus retinitis treated with a ganciclovir implant. Roche Ganciclovir Study Group. N. Engl. J. Med. *340*, 1063–1070.

Mitsuyasu, R.T. (2000). Update on the pathogenesis and treatment of Kaposi sarcoma. Curr. Opin. Oncol. *12*, 174–180.

Montaner, S., Sodhi, A., Pece, S., Mesri, E.A., and Gutkind, J.S. (2001). The Kaposi's sarcoma-associated herpesvirus G protein-coupled receptor promotes endothelial cell survival through the activation of Akt/protein kinase B. Cancer Res. *61*, 2641–2648.

Moore, P.S., and Chang, Y. (2001). Molecular virology of Kaposi's sarcoma-associated herpesvirus. Philos. Trans. R. Soc. Lond. B Biol. Sci. *356*, 499–516.

Muralidhar, S., Pumfery, A.M., Hassani, M., Sadaie, M.R., Kishishita, M., Brady, J.N., Doniger, J., Medveczky, P., and Rosenthal, L.J. (1998). Identification of kaposin (open reading frame K12) as a human herpesvirus 8 (Kaposi's sarcoma-associated herpesvirus) transforming gene. J. Virol. *72*, 4980–4988.

Ong, S.H., Dilworth, S., Hauck-Schmalenberger, I., Pawson, T., and Kiefer, F. (2001). ShcA and Grb2 mediate polyoma middle T antigen-induced endothelial transformation and Gab1 tyrosine phosphorylation. EMBO J. *20*, 6327–6336.

Orsulic, S., Li, Y., Soslow, R.A., Vitale-Cross, L.A., Gutkind, J.S., and Varmus, H.E. (2002). Induction of ovarian cancer by defined multiple genetic changes in a mouse model system. Cancer Cell *1*, 53–62.

Pati, S., Cavrois, M., Guo, H.G., Foulke, J.S., Jr., Kim, J., Feldman, R.A., and Reitz, M. (2001). Activation of NF-κB by the human herpesvirus 8 chemokine receptor ORF74: evidence for a paracrine model of Kaposi's sarcoma pathogenesis. J. Virol. *75*, 8660–8673.

Radkov, S.A., Kellam, P., and Boshoff, C. (2000). The latent nuclear antigen of Kaposi sarcoma-associated herpesvirus targets the retinoblastoma-E2F pathway and with the oncogene Hras transforms primary rat cells. Nat. Med. *6*, 1121–1127.

Rivas, C., Thlick, A.E., Parravicini, C., Moore, P.S., and Chang, Y. (2001). Kaposi's sarcoma-associated herpesvirus LANA2 is a B-cell-specific latent viral protein that inhibits p53. J. Virol. *75*, 429–438.

Russo, J.J., Bohenzky, R.A., Chien, M.C., Chen, J., Yan, M., Maddalena, D., Parry, J.P., Peruzzi, D., Edelman, I.S., Chang, Y., and Moore, P.S. (1996). Nucleotide sequence of the Kaposi sarcoma-associated herpesvirus (HHV8). Proc. Natl. Acad. Sci. USA *93*, 14862–14867.

Sarid, R., Sato, T., Bohenzky, R.A., Russo, J.J., and Chang, Y. (1997). Kaposi's sarcoma-associated herpesvirus encodes a functional bcl-2 homologue. Nat. Med. *3*, 293–298.

Schaefer-Klein, J., Givol, I., Barsov, E.V., Whitcomb, J.M., VanBrocklin, M., Foster, D.N., Federspiel, M.J., and Hughes, S.H. (1998). The EV-O-derived cell line DF-1 supports the efficient replication of avian leukosis-sarcoma viruses and vectors. Virology *248*, 305–311.

Schlaeger, T.M., Bartunkova, S., Lawitts, J.A., Teichmann, G., Risau, W., Deutsch, U., and Sato, T.N. (1997). Uniform vascular-endothelial-cell-specific gene expression in both embryonic and adult transgenic mice. Proc. Natl. Acad. Sci. USA *94*, 3058–3063.

Schwarz, M., and Murphy, P.M. (2001). Kaposi's sarcoma-associated herpesvirus G protein-coupled receptor constitutively activates NF-κB and induces proinflammatory cytokine and chemokine production via a C-terminal signaling determinant. J. Immunol. *167*, 505–513.

Simonart, T., Hermans, P., Schandene, L., and Van Vooren, J.P. (2000). Phenotypic characteristics of Kaposi's sarcoma tumour cells derived from patch-, plaque- and nodular-stage lesions: analysis of cell cultures isolated from AIDS and non-AIDS patients and review of the literature. Br. J. Dermatol. *143*, 557–563.

Sodhi, A., Montaner, S., Patel, V., Zohar, M., Bais, C., Mesri, E.A., and Gutkind, J.S. (2000). The Kaposi's sarcoma-associated herpes virus G protein-coupled receptor up-regulates vascular endothelial growth factor expression and secretion through mitogen-activated protein kinase and p38 pathways acting on hypoxia-inducible factor 1α. Cancer Res. *60*, 4873–4880.

Sodhi, A., Montaner, S., Miyazaki, H., and Gutkind, J.S. (2001). MAPK and Akt act cooperatively but independently on hypoxia inducible factor-1α in rasv12 upregulation of VEGF. Biochem. Biophys. Res. Commun. *287*, 292–300.

Sun, R., Lin, S.F., Staskus, K., Gradoville, L., Grogan, E., Haase, A., and Miller, G. (1999). Kinetics of Kaposi's sarcoma-associated herpesvirus gene expression. J. Virol. *73*, 2232–2242.

Varthakavi, V., Smith, R.M., Deng, H., Sun, R., and Spearman, P. (2002). Human immunodeficiency virus type-1 activates lytic cycle replication of Kaposi's sarcoma-associated herpesvirus through induction of KSHV Rta. Virology *297*, 270–280.

Williams, R.L., Courtneidge, S.A., and Wagner, E.F. (1988). Embryonic lethalities and endothelial tumors in chimeric mice expressing polyoma virus middle T oncogene. Cell *52*, 121–131.

Yang, T.Y., Chen, S.C., Leach, M.W., Manfra, D., Homey, B., Wiekowski, M., Sullivan, L., Jenh, C.H., Narula, S.K., Chensue, S.W., and Lira, S.A. (2000). Transgenic expression of the chemokine receptor encoded by human herpesvirus 8 induces an angioproliferative disease resembling Kaposi's sarcoma. J. Exp. Med. *191*, 445–454.

Yen-Moore, A., Hudnall, S.D., Rady, P.L., Wagner, R.F., Jr., Moore, T.O., Memar, O., Hughes, T.K., and Tyring, S.K. (2000). Differential expression of the HHV-8 vGCR cellular homolog gene in AIDS-associated and classic Kaposi's sarcoma: potential role of HIV-1 Tat. Virology *267*, 247–251.

Yoshida, M. (2001). Multiple viral strategies of HTLV-1 for dysregulation of cell growth control. Annu. Rev. Immunol. *19*, 475–496.

Young, J.A., Bates, P., and Varmus, H.E. (1993). Isolation of a chicken gene that confers susceptibility to infection by subgroup A avian leukosis and sarcoma viruses. J. Virol. *67*, 1811–1816.